



Published in final edited form as:

*Brain Imaging Behav.* 2019 December ; 13(6): 1602–1611. doi:10.1007/s11682-019-00144-1.

## Behavioral inhibition corresponds to white matter fiber bundle integrity in older adults

Paola M. Garcia-Egan<sup>1</sup>, Rebecca N. Preston-Campbell<sup>2</sup>, Lauren E. Salminen<sup>3</sup>, Jodi M. Heaps-Woodruff<sup>2</sup>, Lila Balla<sup>2</sup>, Ryan P. Cabeen<sup>4</sup>, David H. Laidlaw<sup>5</sup>, Thomas E. Conturo<sup>6</sup>, Robert H. Paul<sup>1,2</sup>

<sup>1</sup>Department of Psychological Sciences, University of Missouri, Saint Louis, MO 63121, USA

<sup>2</sup>Missouri Institute of Mental Health, St. Louis, MO 63134, USA

<sup>3</sup>Imaging Genetics Center, Stevens Neuroimaging and Informatics Institute, University of Southern California, Marina del Rey, CA 90292, USA

<sup>4</sup>Laboratory of Neuro Imaging, Stevens Neuroimaging and Informatics Institute, Keck School of Medicine of USC, University of Southern California, Los Angeles, CA, USA

<sup>5</sup>Department of Computer Science, Brown University, Providence, RI, USA

<sup>6</sup>Mallinckrodt Institute of Radiology, Washington University School of Medicine, St. Louis, MO 63110, USA

### Abstract

Little is known about the contribution of white matter integrity to inhibitory cognitive control, particularly in healthy aging. The present study examines the correspondence between white matter fiber bundle length and behavioral inhibition in 37 community-dwelling older adults (aged 51–78 years). Participants underwent neuroimaging with 3 Tesla MRI, and completed a behavioral test of inhibition (i.e., Go/NoGo task). Quantitative tractography derived from diffusion tensor imaging (qtDTI) was used to measure white matter fiber bundle lengths (FBLs) in tracts known to innervate frontal brain regions, including the anterior corpus callosum (AntCC), the cingulate gyrus segment of the cingulum bundle (CING), uncinate fasciculus (UNC), and the superior longitudinal fasciculus (SLF). Performance on the Go/NoGo task was measured by the number of commission errors standardized to reaction time. Hierarchical regression models revealed that shorter FBLs in the CING ( $p < 0.05$ ) and the bilateral UNC ( $p < 0.01$ ) were associated with lower inhibitory performance after adjusting for multiple comparisons, supporting a disconnection model of response inhibition in older adults. Prospective longitudinal studies are needed to examine the evolution of inhibitory errors in older adult populations and potential for therapeutic intervention.

---

Corresponding author: Robert Paul, Ph.D. paulro@umsl.edu, 314 516-8403.

Conflict of interest

Drs. Paul, Heaps, Salminen, Preston-Campbell, Cabeen, Laidlaw, Conturo, and Ms. García-Egan declare no conflicts of interest.

Compliance with Ethical Standards

Informed consent

All procedures were in accordance with the ethical standards of the responsible committee in research involving human subjects (Institutional and national) and with the Helsinki Declaration of 1975, and the applicable revisions at the time of the investigation. Informed consent was obtained from all participants.

## Keywords

Inhibition; Go/NoGo; white matter; quantitative diffusion tensor imaging; MRI fiber bundle length; aging

---

## Introduction

White matter (WM) integrity has been shown to be associated with reduced cognitive function in older adults (Madden, Bennett and Song 2009; Madden et al. 2012). In particular, executive functions that require fast reaction time, such as behavioral inhibition, are vulnerable to age-related compromise (Jacobs et al. 2013; Lee et al. 2012; Lu et al. 2013). Behavioral inhibition refers to the ability to withhold an automatic response, or to resist enticing behaviors (Casey et al. 1997; Menon et al. 2001; Hirose et al. 2012; Dambacher et al. 2014). This higher-order skill in executive function depends on efficient transmission of information across the brain, with predominate involvement of frontal-cortical regions, including the fronto-parietal, fronto-temporal, and frontal-subcortical networks (Rubia et al. 2001; Zhang and Li, 2012; Hong et al. 2016; Steele et al. 2013; van Gaal et al. 2010; Angelini et al. 2015; Garavan et al. 1999).

Studies using MRI diffusion tensor imaging (DTI) reveal that the microstructural integrity of the superior longitudinal fasciculus, uncinate fasciculus (UNC), cingulate gyrus segment of the cingulum, and tracts connecting the inferior frontal gyrus with the subcortical structures, are key anatomical substrates of inhibitory control (Rizk et al. 2017; Sasso et al. 2013; Hinton et al. 2018). Compared to functional neuroimaging measures, indices of structural connectivity (e.g., white matter fractional anisotropy; FA) account for age-related variance in inhibitory performance (Fjell, Sneve, Gryndeland, Storsve and Walhovd 2016).

In previous studies, we described the sensitivity of quantitative diffusion tensor imaging (qDTI) in which we used DTI-based tractography to measure fiber bundle lengths (FBLs) in older individuals (Baker et al. 2014). In this approach, each streamline obtained by tractography is taken to represent a statistical summary of a local bundle of parallel-packed neuronal fibers, from which, the overall arc-length of the trajectory of each fiber bundle is measured (Correia et al. 2008). Additionally, the microstructural properties of the fiber bundles are assessed by measuring the DTI metrics along the entire length of each fiber bundle. This approach combines tractography and DTI scalar metrics to characterize the structural properties of fiber bundles that make up a WM tract. DTI metrics such as FA and mean diffusivity (MD) are usually averaged at the voxel or regional level and single tensor models only measure the directionality of tracts along a primary eigenvector, which lacks information relevant to the organization and microstructure of white matter tracts. In contrast, FBLs are derived from scalar DTI metrics, such as FA, in combination with tractography methods to trace white matter fibers (Correia et al. 2008). Such an approach can detect properties that may be undetected by traditional regional measures of scalar DTI metrics (Correia et al. 2008; Hasan et al. 2009), and reveal additional alterations in white matter integrity that correspond to cognitive decline (Behrman-Lay et al. 2014; Salminen et al. 2016).

Using this approach, older individuals without clinically evident neurodegeneration exhibit reduced FBLs compared to younger adults (Baker et al. 2014; Bolzenius et al. 2013). Moreover, the age-associated shortening of FBL corresponds to worse performance in domains of cognition that are vulnerable to age (Behrman-Lay et al. 2014; Salminen et al. 2013; Salminen et al. 2016; Baker et al. 2017). In particular, we found a relation between shorter FBLs and reduced processing speed (Behrman-Lay et al. 2014; Salminen et al. 2016). To date, no study has utilized the innovative imaging metric of FBL to examine the white matter signature of inhibitory cognitive performance in older adults.

Postmortem studies report reduced length of frontal axonal bundles are reduced in older individuals (Marnier, Nyengaard, Tang and Pakkenberg 2003; Tang, Nyengaard, Pakkenberg and Gundersen 1997), suggesting that alterations in the structural connectome of the brain may underlie an age-related decline in cognitive performance (Behrman-Lay et al. 2014). The present study examined FBLs in four tracts of interest (TOIs) that project to the frontal cortex and have been independently associated with inhibitory control. For example, prior studies using common DTI scalar metrics reveal associations between worse inhibitory performance and lower FA in the anterior corpus callosum (AntCC) and the uncinate fasciculus (UF) (Salo et al. 2009; Hornberger, Geng and Hodges 2011). Higher diffusivity in the cingulate gyrus segment of the cingulum bundle (CING) and the superior longitudinal fasciculus (SLF) also correspond to worse performance on the Go/NoGo task (Colrain et al. 2011; Sasso et al. 2013). Based on our above prior studies of FBL, aging, and cognition, we hypothesized that longer FBLs would correspond with better inhibitory performance.

## Methods

### Participants

A total of 37 healthy older adults between the ages of 51–78 years were included in the study (males  $n = 9$ , females  $n = 28$ ). Participants were all English-speaking individuals and predominantly White/Caucasian ( $n = 26$ , Black/African American  $n = 8$ , and other  $n = 3$ ), with an average education level of 16 years. Exclusion criteria included: 1) a score of  $< 24$  on the Mini-Mental State Examination (MMSE; Folstein, Folstein and McHugh 1975), 2) evidence of neurologic disease, 3) past head injury with loss of consciousness  $> 5$  minutes, 4) severe medical illnesses (e.g., cancer, treatment-dependent diabetes), 4) any Axis I and/or Axis II psychiatric disorders with the exception of treated depression, 5) past or present substance use disorder, 6) any hearing, vision, or motor impairment that precluded cognitive testing, and 7) contraindications for MRI. All participants completed neuropsychological testing within one month of the neuroimaging protocol. The average time between the neuroimaging and neuropsychological evaluations was 23 days. The recruiting methods and total population from which the sample was derived are described in (Paul, et al. 2011). Written informed consent was obtained prior to study participation. Participants received financial compensation for their involvement. The Institutional Review Board at the corresponding universities approved the study.

### Go/NoGo task

A computerized Go/NoGo task was administered in a sound-controlled room. The task required participants to respond repeatedly to target stimuli (Go), and inhibit the prepotent response when non-target stimuli (NoGo) appeared (Beck, Bransome, Mirsky, Rosvold and Sarason 1956). The word “PRESS” was displayed on the screen for 500ms, with a one second inter-stimulus interval. Participants were instructed to press a button with their index finger as quickly as possible when “PRESS” was presented in green font (Go), and to not respond when the word was presented in red font (NoGo). Speed and accuracy of response was equally stressed in the task instructions (Gordon, Cooper, Rennie, Hermens and Williams 2005; Paul et al. 2005). Six trials of 28 stimulus presentations were presented in pseudo-random order, for a total of 168 trials. The ratio of Go to NoGo trials was 75:25. Prior to the task, participants completed a brief practice session. Reaction time was recorded continuously for the duration of the task (6 minutes), but not on a trial-by-trial basis.

To minimize conflation between commission errors and response speed (Bruyer and Brysbaert 2011; Jones et al. 2016; Bezdjan, Baker, Lozano and Raine 2009; Menon et al. 2001; Steele et al. 2013), a composite score of task accuracy and response latency was calculated using the rate residual scoring method (Hirose et al. 2012; Hughes, Linck, Bowles, Koeth and Bunting 2013; Was and Woltz 2007; Woltz and Was 2006). Briefly, a regression line was fit between the average reaction time and the number of false positive errors for all subjects, dividing participants with faster reaction times and fewer errors (below the line = negative scores) from participants with a longer reaction time and/or more errors (above the line = positive scores). The regression line between reaction time and the NoGo errors was used to calculate the inhibitory performance score. The distribution of performances (depicted by dots) represents the distance to the line (Figure 1).

### MRI Data acquisition

All participants were scanned at a single site using a head-only Magnetom Allegra 3T MRI (Siemens Medical Solutions, Erlangen, Germany) with a standard imaging protocol that included a diffusion-weighted MRI sequence. Head positioning was confirmed by a preliminary scout scan composed of three orthogonal planes collected from each individual at the beginning of the scanning procedure. Movement artefact was limited by application of surgical tape across the forehead to enhance stability. High-performance gradients (maximum strength 40 mT/m in a 100-ms rise time; maximum slew rate 400 T/m/s) were utilized to minimize scan times (< 1 hour). FSL BET was used to extract whole brain masks for each subject, and intracranial volume (ICV) was computed from the total volume inside the mask (Jenkinson, Beckmann, Behrens, Woolrich and Smith 2012).

### Diffusion-weighted imaging acquisition

A customized in-house single-shot multislice echo-planar pulse sequence was utilized to acquire the axial diffusion-weighted images. The tensor was encoded using 31 non-collinear directions were utilized, with 24 main directions aligned with the applied diffusion gradient ( $b=996 \text{ s/mm}^2$ ). A “core” of tetrahedral directions (Conturo, McKinstry, Akbudak, and Robinson 1996) was used to maximize the signal-to-noise rate (SNR) efficiency and directional coverage, with 5 baseline  $I_0$  acquisitions ( $b\approx 0$ ). The following parameters were

used: TE=86.2 ms; TR=7.82s; 64 contiguous 2.0-mm slices; and an acquisition matrix of 128 X 128 with a field of view of 256 X 256 mm (isotropic 2.0 X 2.0 X 2.0 mm voxels). Signal was averaged from 72 acquisitions. Further scan acquisition details are described in our prior studies (Baker et al. 2016; Behrman-Lay et al. 2014; Bolzenius et al. 2013; Salminen et al. 2016).

### **Quantitative diffusion tractography (qtDTI)**

Diffusion-weighted volumes were preprocessed using FSL 5.0 (Jenkinson et al. 2012) and the Quantitative Imaging Toolkit (QIT) (Cabeen, Laidlaw and Toga 2018). The images were corrected for motion and eddy-current induced artifacts through affine registration to the first baseline volume using FSL FLIRT (Jenkinson and Smith 2001) with the mutual information criteria. The orientations of the gradient encoding directions were corrected by the rotation induced by these registrations (Leemans and Jones 2009), and brain tissue was extracted using FSL BET (Smith 2002) with a fraction threshold of 0.45. Diffusion tensor images were estimated for each subject using FSL DTIFIT and a study-specific white matter atlas was created using DTI-TK (Zhang, Yushkevich, Rueckert and Gee 2007). The template image was computed by iteratively deforming and averaging the sample imaging data using the tensor-based deformable registration algorithm in DTI-TK (Zhang, Yushkevich, Alexander and Gee 2006) with finite strain tensor reorientation and the deviatoric tensor similarity metric. This template was used to define the AntCC, bilateral CING, bilateral UF, and bilateral SLF (Mori and van Zijl 2002).

Specificity of fiber extraction is difficult without tractography maps, due the heterogeneity and convoluted nature of WM bundles. Therefore, we used a template-based approach to extract subject-specific fiber bundle models; specifically, whole brain tractography was performed in the subject native space, and subsets of curves were selected using template masks to select each bundle-of-interest (Zhang et al. 2010). For each bundle-of-interest, two inclusion region of interests (ROIs) and one exclusion ROI were drawn in template space using ITK-SNAP (Yushkevich et al. 2006). These masks were placed at opposite ends of each bundle, and then drawn in reference to standard white matter atlases (Catani and de Schotten 2012). Tractography was performed in subject native space using deterministic streamline integration using QIT (Zhang, Demiralp and Laidlaw 2003) with a step size of 1 mm, tricubic interpolation, and four jittered seeds per voxel. Termination criteria included an angle threshold of 45 degrees and minimum FA of 0.15. Fiber curves with lengths less than 10 mm were excluded from the analysis. FBLs were computed from the resulting curves (Correia et al. 2008). Corrections for head size were made by dividing FLB measures by the ratio of participants' ICV to the sample average ICV (Correia et al. 2008). Representation of TOIs is shown in Figure 2.

### **Statistical Analyses**

Statistical analyses were conducted in SPSS 25 (IBM Corp 2017). The Shapiro-Wilk Tests of normality were performed, and skewness and kurtosis scores were evaluated to assess for normal distribution of the data. Group differences in age and education between “good” and “poor” performers were examined using independent-samples t-tests; Chi-square tests examined differences in sex and ethnicity. Preliminary analyses revealed skewed

distributions for age, reaction time, omission errors, inhibitory errors, AntCC, SLF and CING, therefore, the  $p$ -value was calculated based on 1000 bootstraps to correct for potential deviation from the Gaussian distribution (Pavlov, Wilson, Delgado 2010; Haukoos and Lewis 2008). The Shapiro-Wilk test ( $p = 0.53$ ) revealed that the distribution of inhibitory performance scores was similar to a Gaussian distribution; the SD of the distribution of the inhibitory performance score was 0.97 (Figure 3). The purpose of correlations analysis was to establish whether age and education should be included in the regression model, correlations were conducted to examine associations with TOIs.

Inspection of diagnostic plots (Q–Q plots and residual plots) and diagnostic statistical values (Cook's distance  $< 1$ , variance inflation factor  $< 4$ ) revealed no violations of the statistical assumptions. As such, hierarchical regression analysis was used to determine the association between the composite score of inhibitory performance on the Go/NoGo task with each TOI. To address whether specific TOIs were associated significantly with Go/NoGo performance after adjusting for age, we conducted structured hierarchical regression models for each TOI, with age in the first block, and inhibitory performance entered in the second block. The data are presented as mean  $\pm$  standard deviation (SD) or median and interquartile range (IQR) for non-normal distributed variables. Bootstrapped significance was set as  $p < 0.05$ . The False Discovery Rate (FDR) procedure was used to correct for multiple comparisons (Benjamini and Hochberg 1995).

## Results

Demographic characteristics of the sample are reported in Table 1. Results of the correlations showed a relationship between inhibitory performance and FBL in the CING and the UNC (Table 2). However, no association between age and TOIs, and education and TOIs emerged. Results of the hierarchical structured regression revealed that inhibitory performance was significantly associated with FBLs in the CING (Adjusted  $R^2 = 0.124$ ;  $p = 0.021$ ) and the UNC (Adjusted  $R^2 = 0.247$ ;  $p = 0.006$ ) after FDR corrections, but not with the AntCC (Adjusted  $R^2 = 0.103$ ;  $p = 0.114$ ) and SLF (Adjusted  $R^2 = 0.145$ ;  $p = 0.083$ ) (Table 3).

## Discussion

This is the first study using qtDTI to investigate the white matter substrate of inhibition in healthy older adults. Our results show that shorter FBL of the UNC tract and the CING correlate with lower inhibitory performance, when accounting for speed-accuracy trade-offs. These results provide empirical support for a disconnection model of inhibition in a healthy aging population (Greenwood 2000; O'Sullivan et al. 2001; Charlton et al. 2006; Madden et al. 2017; Fjell, Sneve, Grydeland, Storsve and Walhovd 2017; Salat et al. 2005).

The association between inhibition and the UNC in the present study is noteworthy. The UNC connects the frontal lobe (primarily the orbitofrontal cortex) to the anterior temporal lobe, including the amygdala and hippocampus (Kier, Staib, Davis and Bronen 2004). In healthy adults, lower performance on the Go/NoGo and Stroop tests are significantly associated with decreased WM microstructural integrity of the UNC (Sasson et al. 2013).



These results provide empirical support for a disconnection model of inhibition in a healthy aging population (Greenwood 2000; O'Sullivan et al. 2001; Charlton et al. 2006; Madden et al. 2017; Fjell et al. 2017; Salat et al. 2005). The disconnection theory of aging proposes that age-related cognitive decline results predominately from degenerated connections between cortical regions rather than focal degeneration within a cortical region. Between the ages of 20 through 80, myelinated fibers are shortened by 50% (Marner et al. 2003). It is estimated that these fibers shorten at a rate of 10% per decade (Tang et al. 1997). Shortened axon bundles are believed to underlie mechanisms of age-related cognitive decline (Catani 2006).

The observation that FBL in the CING corresponds to inhibition is consistent with prior studies in healthy participants (Rizk et al. 2017; Metzler-Baddeley et al. 2012), as well as clinical populations (Murphy et al. 2008, Kubicki et al. 2014, Hornberger, Geng and Hodges 2011). Anatomically, the CING is connected to frontal, parietal, and medial temporal sites, as well as subcortical nuclei (Schmahmann and Pandya 2006), all of which are essential for executive control (self-monitoring and evaluation of performance) and processing speed (Yang et al. 2016; Sasson et al. 2013).

Axonal degeneration among generally healthy older adults is likely associated with demyelination secondary to inflammation and oxidative stress (Pan and Chan 2017). As reflected in studies with healthy older adults, decreased FA and increased MD are common findings in studies of older brains (Inano, Takao, Hayashi, Abe and Ohtomo 2011; Bennett, Madden, Vaidya, Howard and Howard 2010; Westlye et al. 2009; Sexton et al. 2014; Bender, Völkle and Raz 2016; Charlton, Schiavone, Barrick, Morris and Markus 2010). These age effects are probably driven by changes in underlying myelin, as suggested by consistently shown age-related increases in radial diffusivity, whereas axial diffusivity changes less consistently observed (Sullivan et al. 2010; Zahr, Rohlfing, Pfefferbaum and Sullivan 2009; Davis et al., 2009; Phillips et al. 2013; Inano et al. 2011). More studies using advanced microstructural modeling techniques, such as Neurite Orientation Dispersion and Density Imaging (Zhang, Schneider, Wheeler-Kingshott, and Alexander 2012) are needed to address this question.

Although there is increasing interest in qtDTI, we acknowledge there are some limitations related to this technique. We used affine registration, which may have resulted in missed fibers or the inclusion of extra fibers that terminate at regions distant from the WM-gray matter boundary. Complex WM configurations are not well characterized by single-tensor modeling, and multi-compartment diffusion may offer more anatomically accurate results (Cabeen, Bastin and Laidlaw 2016). Similarly, the anatomical precision of FBLs could be enhanced by high angular resolution diffusion. The age of the sample was fairly young and the range was limited, which may have accounted for the absence of a clear age effect. Furthermore, our sample was relatively small and may not be representative of the population. Longitudinal studies utilizing multiple measures of inhibitory control in a larger sample of older individuals are needed to the generalizability of the results in other elderly cohorts.

## Conclusion

The present study revealed that WM integrity of the UNC and left CING correspond to behavioral inhibition among healthy older adults. The results support a disconnection model of cognitive aging. Additional studies using a prospective design are needed to define the development of inhibitory performance errors in older adults and determine the real-world relevance of such errors in everyday living skills.

## Acknowledgments

### Funding

Supported by National Institutes of Health/National Institute of Neurological Disorders and Stroke grant number R01 NS052470 and R01 NS039538, National Institutes of Health/National Institute of Mental Health grant R21 MH090494.

## References

- Angelini M, Calbi M, Ferrari A, Sbriscia-Fioretti B, Franca M, Gallese V, & Umiltà MA (2015). Motor inhibition during overt and covert actions: An electrical neuroimaging study. *PLoS ONE*, 10(5). 10.1371/journal.pone.0126800
- Baker LM, Cabeen RP, Cooley SA, Laidlaw DH, & Paul RH (2016). Application of a novel quantitative tractography-based analysis of diffusion tensor imaging to examine fiber bundle length in human cerebral white matter. *Technology and Innovation*, 18, 21–29. [PubMed: 27721932]
- Baker LM, Laidlaw DH, Conturo TE, Hogan J, Zhao Y, Luo X, et al. (2014). White matter changes with age utilizing quantitative diffusion MRI. *Neurology*, 83(3), 247–252. [PubMed: 24928121]
- Baker LM, Laidlaw DH, Cabeen R, Akbudak E, Conturo TE, Correia S, ... & Salminen LE (2017). Cognitive reserve moderates the relationship between neuropsychological performance and white matter fiber bundle length in healthy older adults. *Brain imaging and behavior*, 11(3), 632–639. [PubMed: 26961092]
- Beck LH, Bransome ED Jr., Mirsky AF, Rosvold HE, & Sarason I (1956). A continuous performance test of brain damage. *Journal of Consulting Psychology*, 20(5), 343–350. [PubMed: 13367264]
- Behrman-Lay AM, Usher C, Conturo TE, Correia S, Laidlaw DH, Lane EM, et al. (2014). Fiber bundle length and cognition: a length-based tractography MRI study. *Brain Imaging and Behavior*. 9(4), 765–775.
- Bender AR, Völkle MC, & Raz N (2016). Differential aging of cerebral white matter in middle-aged and older adults: a seven-year follow-up. *Neuroimage*, 125, 74–83. [PubMed: 26481675]
- Benjamini Y, & Hochberg Y (1995). Controlling the false discovery rate: a practical and powerful approach to multiple testing. *Journal of the royal statistical society. Series B (Methodological)*, 289–300.
- Bennett IJ, Madden DJ, Vaidya CJ, Howard JH Jr, & Howard DV (2011). White matter integrity correlates of implicit sequence learning in healthy aging. *Neurobiology of Aging*, 32(12), 2317–e1.
- Bezdjian S, Baker LA, Lozano DI, & Raine A (2009). Assessing inattention and impulsivity in children during the Go/NoGo task. *British Journal of Developmental Psychology*, 27(2), 365–383. [PubMed: 19812711]
- Bolzenius JD, Laidlaw DH, Cabeen RP, Conturo TE, McMichael AR, Lane EM, et al. (2013). Impact of body mass index on neuronal fiber bundle lengths among healthy older adults. *Brain Imaging Behavior*, 7(3), 300–306. [PubMed: 23564371]
- Bruyer R, & Brysbaert M (2011). Combining speed and accuracy in cognitive psychology: Is the inverse efficiency score (IES) a better dependent variable than the mean reaction time (RT) and the percentage of errors (PE)? *Psychologica Belgica*, 51(1), 5–13.
- Cabeen RP, Bastin ME, & Laidlaw DH (2016). Kernel regression estimation of fiber orientation mixtures in diffusion MRI. *Neuroimage*, 127, 158–172. [PubMed: 26691524]



- Cabeen RP, Laidlaw DH, & Toga AW (2018). Quantitative Imaging Toolkit: Software for Interactive 3D Visualization, Data Exploration, and Computational Analysis of Neuroimaging Datasets. In Proceedings of the Joint Annual Meeting ISMRM-ESMRMB Paris, France (p. 2854).
- Casey BJ, Trainor RJ, Orendi JL, Schubert AB, Nystrom LE, Giedd JN, et al. (1997). A developmental functional MRI study of prefrontal activation during performance of a Go-No-Go task. *Journal of Cognitive Neuroscience*, 9(6), 835–847. [PubMed: 23964603]
- Catani M (2006). Diffusion tensor magnetic resonance imaging tractography in cognitive disorders. *Current opinion in neurology*, 19(6), 599–606. [PubMed: 17102700]
- Catani M, & de Schotten MT (2012). *Atlas of Human Brain Connections*. Oxford University Press.
- Charlton RA, Barrick TR, McIntyre DJ, Shen Y, O'sullivan M, Howe FEEA, et al. (2006). White matter damage on diffusion tensor imaging correlates with age-related cognitive decline. *Neurology*, 66(2), 217–222. [PubMed: 16434657]
- Colrain IM, Sullivan EV, Ford JM, Mathalon DH, McPherson S-L, Roach BJ, et al. (2011). Frontally mediated inhibitory processing and white matter microstructure: age and alcoholism effects. *Psychopharmacology*, 213(4), 669–679. [PubMed: 21161189]
- Conturo TE, McKinsty RC, Akbudak E, & Robinson BH (1996). Encoding of anisotropic diffusion with tetrahedral gradients: a general mathematical diffusion formalism and experimental results. *Magnetic Resonance in Medicine*, 35(3), 399–412. [PubMed: 8699953]
- Corp, I. B. M. (2017). *IBM SPSS statistics for windows, version 25.0*. Armonk, NY: IBM Corp.
- Correia S, Lee SY, Voorn T, Tate DF, Paul RH, Zhang S, et al. (2008). Quantitative tractography metrics of white matter integrity in diffusion-tensor MRI. *Neuroimage*, 42(2), 568–581. [PubMed: 18617421]
- Dambacher F, Sack AT, Lobbstael J, Arntz A, Brugmann S, & Schuhmann T (2014). The role of right prefrontal and medial cortex in response inhibition: Interfering with action restraint and action cancellation using transcranial magnetic brain stimulation. *Journal of Cognitive Neuroscience*, 26(8), 1775–1784. 10.1162/jocn\_a\_00595 [PubMed: 24564464]
- Davis SW, Dennis NA, Buchler NG, White LE, Madden DJ, & Cabeza R (2009). Assessing the effects of age on long white matter tracts using diffusion tensor tractography. *Neuroimage*, 46(2), 530–541. [PubMed: 19385018]
- Fjell AM, Sneve MH, Grydeland H, Storsve AB, & Walhovd KB (2016). The disconnected brain and executive function decline in aging. *Cerebral Cortex*, 27(3), 2303–2317.
- Folstein MF, Folstein SE, & McHugh PR (1975). "Mini-mental state": a practical method for grading the cognitive state of patients for the clinician. *Journal of Psychiatric Research*, 12(3), 189–198. [PubMed: 1202204]
- Garavan H, Ross TJ, & Stein EA (1999). Right hemispheric dominance of inhibitory control: an event-related functional MRI study. *Proceedings of the National Academy of Science of the USA*, 96(14), 8301–8306.
- Gordon E, Cooper N, Rennie C, Hermens D, & Williams LM (2005). Integrative neuroscience: The role of a standardized database. *Clinical EEG and Neuroscience*, 36(2), 64–75. [PubMed: 15999901]
- Greenwood PM (2000). The frontal aging hypothesis evaluated. *Journal of the International Neuropsychological Society*, 6(6), 705–726. [PubMed: 11011517]
- Hasan KM, Iftikhar A, Kamali A, Kramer LA, Ashtari M, Cirino PT, et al. (2009). Development and aging of the healthy human brain uncinate fasciculus across the lifespan using diffusion tensor tractography. *Brain Research*, 1276, 67–76. [PubMed: 19393229]
- Haukoos JS, & Lewis RJ (2005). Advanced statistics: Bootstrapping confidence intervals for statistics with "difficult" distributions. *Academic Emergency Medicine*, 12(4), 360–365. [PubMed: 15805329]
- Hinton KE, Lahey BB, Villalta-Gil V, Boyd BD, Yvernault BC, Werts KB, et al. (2018). Right fronto-subcortical white matter microstructure predicts cognitive control ability on the Go/No-go task in a community sample. *Frontiers in Human Neuroscience*, 12, 127. [PubMed: 29706875]
- Hirose S, Chikazoe J, Watanabe T, Jimura K, Kunimatsu A, Abe O, et al. (2012). Efficiency of Go/No-Go task performance implemented in the left hemisphere. *Journal of Neuroscience*, 32(26), 9059–9065. [PubMed: 22745505]

- Hong X, Liu Y, Sun J, & Tong S (2016). Age-related differences in the modulation of small-world brain networks during a Go/NoGo task. *Frontiers in Aging Neuroscience*, 8, 100. [PubMed: 27242512]
- Hornberger M, Geng J, & Hodges JR (2011). Convergent grey and white matter evidence of orbitofrontal cortex changes related to disinhibition in behavioural variant frontotemporal dementia. *Brain*, 134(9), 2502–2512. [PubMed: 21785117]
- Hughes MM, Linck JA, Bowles AR, Koeth JT, & Bunting MF (2014). Alternatives to switch-cost scoring in the task-switching paradigm: Their reliability and increased validity. *Behavior Research Methods*, 46(3), 702–721. [PubMed: 24356991]
- Inano S, Takao H, Hayashi N, Abe O, & Ohtomo K (2011). Effects of age and gender on white matter integrity. *American Journal of Neuroradiology*, 32(100), 2103–2109. [PubMed: 21998104]
- Jacobs HI, Leritz EC, Williams VJ, Van Boxel MP, van der Elst W, Jolles J, et al. (2013). Association between white matter microstructure, executive functions, and processing speed in older adults: The impact of vascular health. *Human Brain Mapping*, 34(1), 77–95. [PubMed: 21954054]
- Jenkinson M, Beckmann CF, Behrens TE, Woolrich MW, & Smith SM (2012). Fsl. *Neuroimage*, 62(2), 782–790. [PubMed: 21979382]
- Jenkinson M, & Smith S (2001). A global optimisation method for robust affine registration of brain images. *Medical Image Analysis*, 5(2), 143–156. [PubMed: 11516708]
- Jones SA, Butler BC, Kintzel F, Johnson A, Klein RM, & Eskes GA (2016). Measuring the performance of attention networks with the Dalhousie computerized attention battery (DalCAB): Methodology and reliability in healthy adults. *Frontiers in Psychology*, 7, 823. [PubMed: 27375517]
- Kier EL, Staib LH, Davis LM, & Bronen RA (2004). MR imaging of the temporal stem: anatomic dissection tractography of the uncinate fasciculus, inferior occipitofrontal fasciculus, and Meyer's loop of the optic radiation. *American Journal of Neuroradiology*, 25(5), 677–691. [PubMed: 15140705]
- Kubicki M, Niznikiewicz M, Connor E, Ungar L, Nestor P, Bouix S, et al. (2009). Relationship between white matter integrity, attention, and memory in schizophrenia: A diffusion tensor imaging study. *Brain Imaging and Behavior*, 3(2), 191–201. [PubMed: 20556231]
- Lee T, Mosing MA, Henry JD, Trollor JN, Lammell A, Ames D, et al. (2012). Genetic influences on five measures of processing speed and their covariation with general cognitive ability in the elderly: The older Australian twins study. *Behavior Genetics*, 42(1), 96–106. [PubMed: 21617952]
- Leemans A, & Jones DK (2009). The B-matrix must be rotated when correcting for subject motion in DTI data. *Magnetic Resonance in Medicine*, 61(6), 1336–1349. [PubMed: 19319973]
- Lu PH, Lee GJ, Tishler TA, Meghpara M, Thompson PM, & Bartzokis G (2013). Myelin breakdown mediates age-related slowing in cognitive processing speed in healthy older men. *Brain and Cognition*, 81(1), 131–138. [PubMed: 23195704]
- Madden DJ, Bennett IJ, & Song AW (2009). Cerebral white matter integrity and cognitive aging: contributions from diffusion tensor imaging. *Neuropsychology review*, 19(4), 415–35. [PubMed: 19705281]
- Madden DJ, Bennett IJ, Burzynska A, Potter GG, Chen NK, & Song AW (2012). Diffusion tensor imaging of cerebral white matter integrity in cognitive aging. *Biochimica et biophysica acta*, 1822(3), 386–400. [PubMed: 21871957]
- Madden DJ, Parks EL, Tallman CW, Boylan MA, Hoagey DA, Cocjin SB, et al. (2017). Sources of disconnection in neurocognitive aging: cerebral white-matter integrity, resting-state functional connectivity, and white-matter hyperintensity volume. *Neurobiology of Aging*, 54, 199–213. [PubMed: 28389085]
- Marner L, Nyengaard JR, Tang Y, & Pakkenberg B (2003). Marked loss of myelinated nerve fibers in the human brain with age. *Journal of comparative neurology*, 462(2), 144–152. [PubMed: 12794739]
- Menon V, Adleman NE, White CD, Glover GH, & Reiss AL (2001). Error-related brain activation during a Go/NoGo response inhibition task. *Human Brain Mapping*, 12(3), 131–143. [PubMed: 11170305]

- Mettenburg JM, Benzinger TLS, Shimony JS, Snyder AZ, & Sheline YI (2012). Diminished performance on neuropsychological testing in late life depression is correlated with microstructural white matter abnormalities. *Neuroimage*, 60(4), 2182–2190. [PubMed: 22487548]
- Metzler-Baddeley C, Jones DK, Steventon J, Westacott L, Aggleton JP, & O’Sullivan MJ (2012). Cingulum microstructure predicts cognitive control in older age and mild cognitive impairment. *Journal of Neuroscience*, 32(49), 17612–17619. [PubMed: 23223284]
- Mori S, & van Zijl PC (2002). Fiber tracking: principles and strategies - a technical review. *NMR Biomedicine*, 15(7–8), 468–480.
- Murphy CF, Gunning-Dixon FM, Hoptman MJ, Lim KO, Ardekani B, Shields JK, et al. (2007). White-matter integrity predicts stroop performance in patients with geriatric depression. *Biological psychiatry*, 61(8), 1007–1010. [PubMed: 17123478]
- O’Sullivan MRCP, Jones DK, Summers PE, Morris RG, Williams SCR, & Markus HS (2001). Evidence for cortical “disconnection” as a mechanism of age-related cognitive decline. *Neurology*, 57(4), 632–638. [PubMed: 11524471]
- Pan S, & Chan JR (2017). Regulation and dysregulation of axon infrastructure by myelinating glia. *J Cell Biol*, 216(12), 3903–3916. [PubMed: 29114067]
- Pavlov IY, Wilson AR, & Delgado JC (2010). Resampling approach for determination of the method for reference interval calculation in clinical laboratory practice. *Clinical and Vaccine Immunology*, 17(8), 1217–1222. [PubMed: 20554803]
- Paul R, Lane EM, Tate DF, Heaps J, Romo DM, Akbudak E, et al. (2011). Neuroimaging signatures and cognitive correlates of the Montreal cognitive assessment screen in a nonclinical elderly sample. *Archives of Clinical Neuropsychology*, 26(5), 454–460. [PubMed: 21642663]
- Paul RH, Lawrence J, Williams LM, Richard CC, Cooper N, & Gordon E (2005). Preliminary validity of “integneuro”: a new computerized battery of neurocognitive tests. *International Journal of Neuroscience*, 115(11), 1549–1567.
- Phillips OR, Clark KA, Luders E, Azhir R, Joshi SH, Woods RP, et al. (2013). Superficial white matter: effects of age, sex, and hemisphere. *Brain Connectivity*, 3(2), 146–159. [PubMed: 23461767]
- Rizk MM, Rubin-Falcone H, Keilp J, Miller JM, Sublette ME, Burke A, et al. (2017). White matter correlates of impaired attention control in major depressive disorder and healthy volunteers. *Journal of Affective Disorders*, 222, 103–111. [PubMed: 28688263]
- Rubia K, Russell T, Overmeyer S, Brammer MJ, Bullmore ET, Sharma T, et al. (2001). Mapping motor inhibition: conjunctive brain activations across different versions of go/no-go and stop tasks. *Neuroimage*, 13(2), 250–261. [PubMed: 11162266]
- Salat DH, Tuch DS, Greve DN, Van Der Kouwe AJW, Hevelone ND, Zaleta AK, et al. (2005). Age-related alterations in white matter microstructure measured by diffusion tensor imaging. *Neurobiology of Aging*, 26(8), 1215–1227. [PubMed: 15917106]
- Salminen LE, Schofield PR, Lane EM, Heaps JM, Pierce KD, Cabeen R, ... & Paul RH (2013). Neuronal fiber bundle lengths in healthy adult carriers of the ApoE4 allele: a quantitative tractography DTI study. *Brain imaging and behavior*, 7(3), 274–281. [PubMed: 23475756]
- Salminen LE, Schofield PR, Pierce KD, Zhao Y, Luo X, Wang Y, et al. (2016). Neuromarkers of the common angiotensinogen polymorphism in healthy older adults: A comprehensive assessment of white matter integrity and cognition. *Behavioural Brain Research*, 296, 85–93.
- Salo R, Nordahl TE, Buonocore MH, Natsuaki Y, Waters C, Moore CD, et al. (2009). Cognitive control and white matter callosal microstructure in methamphetamine dependent subjects: A DTI study. *Biological Psychiatry*, 65(2), 122–128. [PubMed: 18814867]
- Sasson E, Doniger GM, Pasternak O, Tarrasch R, & Assaf Y (2013). White matter correlates of cognitive domains in normal aging with diffusion tensor imaging. *Frontiers in Neuroscience*, 7, 32. [PubMed: 23493587]
- Schmahmann JD, & Pandya DN (2006). *Fiber Pathways of the Brain*. Oxford University Press New York.
- Sexton CE, Walhovd KB, Storsve AB, Tamnes CK, Westlye LT, Johansen-Berg H, & Fjell AM (2014). Accelerated changes in white matter microstructure during aging: a longitudinal diffusion tensor imaging study. *Journal of Neuroscience*, 34(46), 15425–15436. [PubMed: 25392509]

- Smith SM (2002). Fast robust automated brain extraction. *Human Brain Mapping*, 17(3), 143–155. [PubMed: 12391568]
- Steele VR, Aharoni E, Munro GE, Calhoun VD, Nyalakanti P, Stevens MC, et al. (2013). A large scale (N = 102) functional neuroimaging study of response inhibition in a Go/NoGo task. *Behavioural Brain Research*, 256, 529–536. [PubMed: 23756137]
- Sullivan EV, Rohlfing T, & Pfefferbaum A (2010). Quantitative fiber tracking of lateral and interhemispheric white matter systems in normal aging: relations to timed performance. *Neurobiology of Aging*, 31(3), 464–481. [PubMed: 18495300]
- Tang Y, Nyengaard JR, Pakkenberg B, & Gundersen HJG (1997). Age-induced white matter changes in the human brain: a stereological investigation. *Neurobiology of aging*, 18(6), 609–615. [PubMed: 9461058]
- van Gaal S, Ridderinkhof KR, Scholte HS, & Lamme VAF (2010). Unconscious activation of the prefrontal No-Go network. *Journal of Neuroscience*, 30(11), 4143–4150. [PubMed: 20237284]
- Was CA, & Woltz DJ (2007). Reexamining the relationship between working memory and comprehension: The role of available longterm memory. *Journal of Memory and Language*, 56(1), 86–102.
- Westlye LT, Walhovd KB, Dale AM, Bjørnerud A, Due-Tønnessen P, Engvig A, et al. (2009). Life-span changes of the human brain white matter: diffusion tensor imaging (DTI) and volumetry. *Cerebral Cortex*, 20(9), 2055–2068. [PubMed: 20032062]
- Woltz DJ, & Was CA (2006). Availability of related long-term memory during and after attention focus in working memory. *Memory & Cognition*, 34(3), 668–684. [PubMed: 16933773]
- Yang J, Tian X, Wei D, Liu H, Zhang Q, Wang K, et al. (2016). Macro and micro structures in the dorsal anterior cingulate cortex contribute to individual differences in self-monitoring. *Brain Imaging and Behavior*, 10(2), 477–485. [PubMed: 25958159]
- Yushkevich PA, Piven J, Hazlett HC, Smith RG, Ho S, Gee JC, et al. (2006). User-guided 3D active contour segmentation of anatomical structures: significantly improved efficiency and reliability. *Neuroimage*, 31(3), 1116–1128. [PubMed: 16545965]
- Zhang H, Yushkevich PA, Alexander DC, & Gee JC (2006). Deformable registration of diffusion tensor MR images with explicit orientation optimization. *Medical Image Analysis*, 10(5), 764–785. [PubMed: 16899392]
- Zhang H, Yushkevich PA, Rueckert D, & Gee JC (2007, 10). Unbiased white matter atlas construction using diffusion tensor images. In *International Conference on Medical Image Computing and Computer-Assisted Intervention* (pp. 211–218). Springer, Berlin, Heidelberg.
- Zhang S, Demiralp C, & Laidlaw DH (2003). Visualizing diffusion tensor MR images using streamtubes and streamsurfaces. *IEEE Transactions on Visualization and Computer Graphics*, 9(4), 454–462.
- Zhang H, Schneider T, Wheeler-Kingshott CA, & Alexander DC (2012). NODDI: practical in vivo neurite orientation dispersion and density imaging of the human brain. *Neuroimage*, 61(4), 1000–1016. [PubMed: 22484410]
- Zhang S, & Li CR (2012). Functional networks for cognitive control in a stop signal task: Independent component analysis. *Human Brain Mapping*, 33(1), 89–104. [PubMed: 21365716]
- Zhang Y, Zhang J, Oishi K, Faria AV, Jiang H, Li X, ... & Toga AW (2010). Atlas-guided tract reconstruction for automated and comprehensive examination of the white matter anatomy. *Neuroimage*, 52(4), 1289–1301 [PubMed: 20570617]

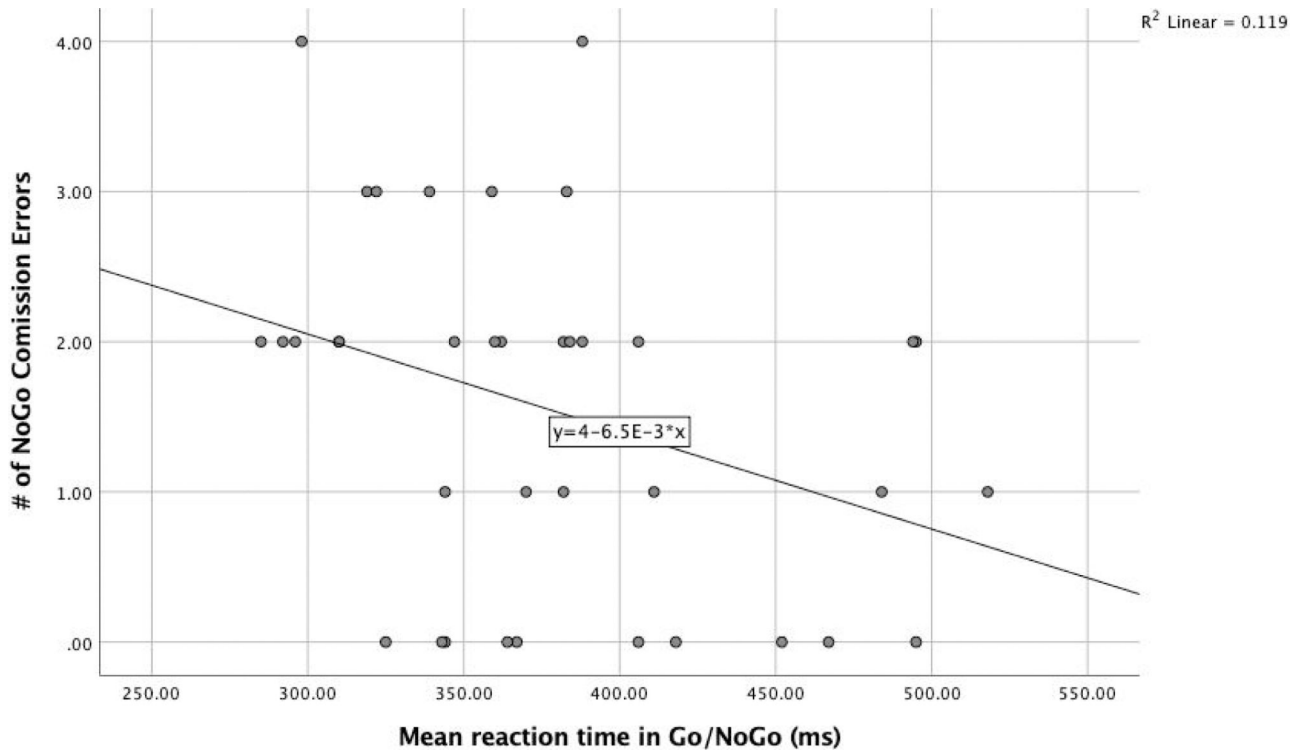


**Fig. 1.**  
Regression of overall reaction time and commission errors

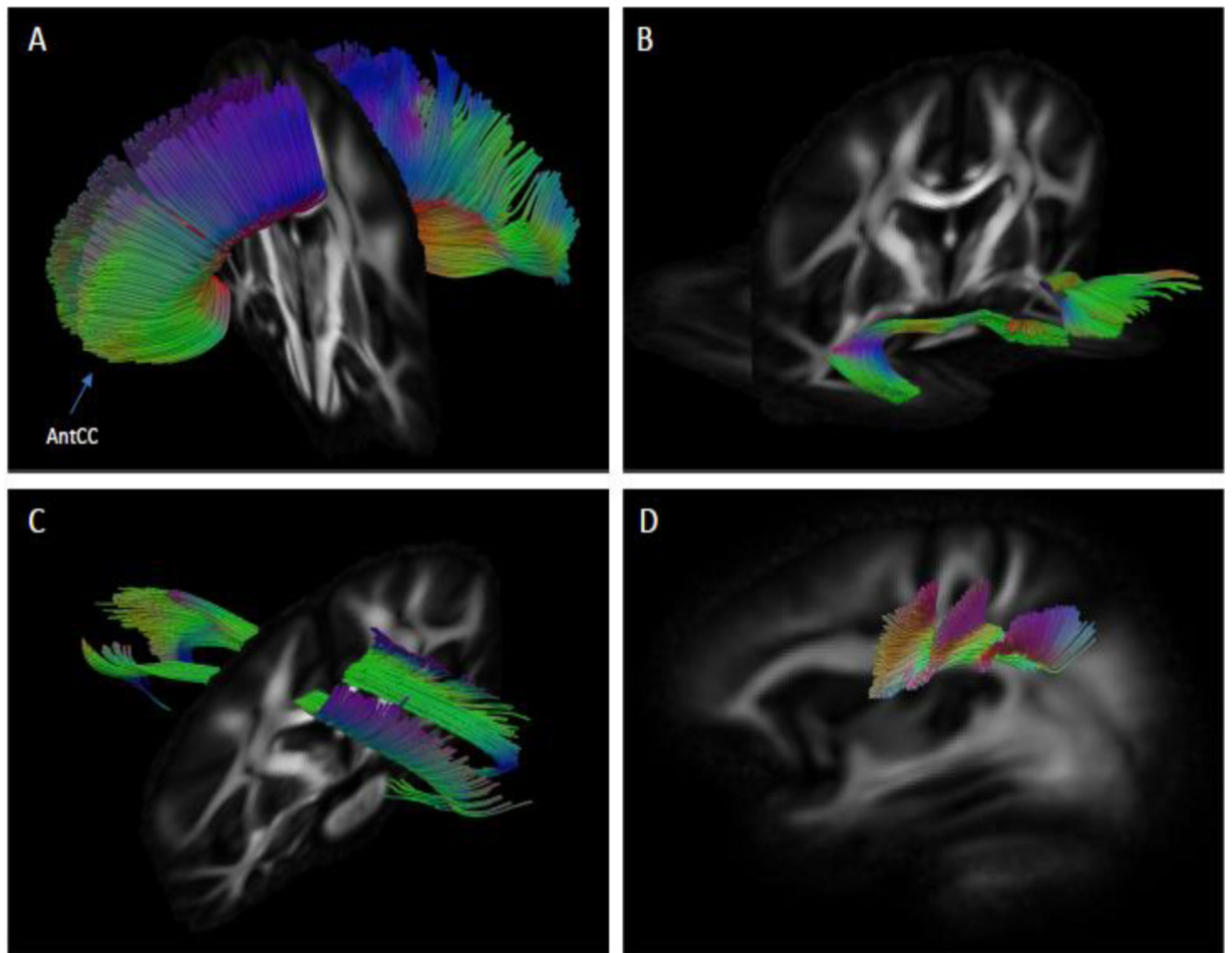


**Fig 2.** Reconstruction of white matter tracts of interest using qtDTI in coronal plane view: A) Anterior corpus callosum (AntCC). B) Uncinate fasciculus. C) Cingulum bundle. In sagittal plane view: D) Superior longitudinal fasciculus.



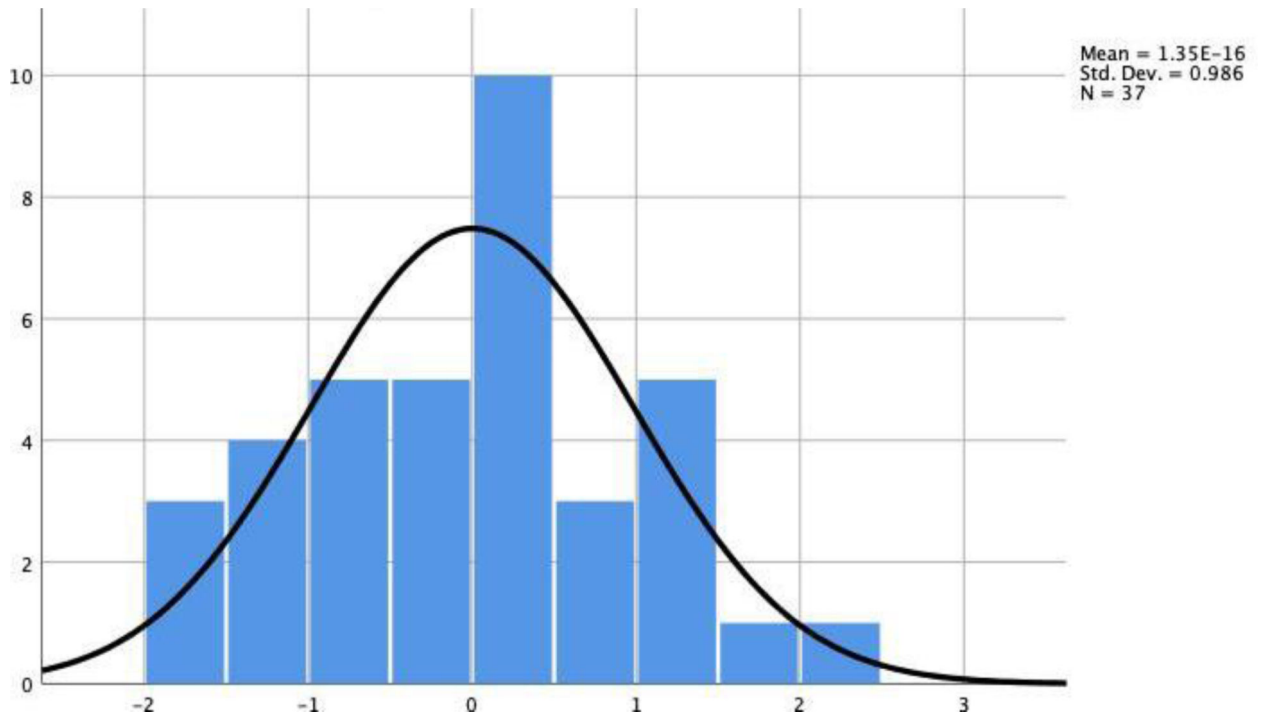


**Fig 3.**  
Distribution of regression standardized values as efficiency index scores

Author Manuscript

Author Manuscript

Author Manuscript

Author Manuscript

**Table 1.**

Demographic information, cognition and mean fiber bundle length (mm) in the sample (N=37)

Variable	Mean/Median	SD/IQR	Minimum	Maximum
Demographics				
Age	59.00	12.50	51	78
Education	15.81	2.38	12	20
Cognition				
MMSE	28.84	1.67	26	30
Go/NoGo Reaction Time (ms)	367.00	76.50	285	518
Commission (NoGo) Errors	2.00	2	0	4
Omission (Go) Errors	1	2.5	0	24
Fiber bundle lengths				
Anterior corpus callosum	99.79	15.33	70.87	154.34
Cingulum	86.05	17.31	61.21	125.70
Uncinate Fasciculus	66.55	12.89	39.14	95.69
Superior longitudinal fasciculus	68.37	11.13	53.21	98.97

Fiber bundle lengths corrected for head size, SD: standard deviation, IQR: interquartile range, MMSE: Mini-Mental State Examination.

**Table 2.**

Correlations of mean fiber bundle length, demographics, and efficiency score index

Variables	AntCC <i>r</i>	CING <i>r</i>	UF <i>r</i>	SLF <i>r</i>
Age	-0.167	-0.091	0.057	-0.131
Education	-0.013	-0.073	-0.244	-0.026
Inhibitory performance score	-0.286	-0.411 *	-0.497 **	-0.366

\*  
 $p < 0.05$ \*\*  
 $p = < 0.01$ .

Author Manuscript

Author Manuscript

Author Manuscript

Author Manuscript

Hierarchical multiple regression models of qDTI metrics of 4 TOIs and efficiency index scores when controlling for age

**Table 3.**

Predictor	Anterior corpus callosum				Cingulum				Uncinate fasciculus				Superior longitudinal fasciculus			
	R <sup>2</sup> change	F change	$\beta$	SE	R <sup>2</sup> change	F change	$\beta$	SE	R <sup>2</sup> change	F change	$\beta$	SE	R <sup>2</sup> change	F change	$\beta$	SE
Step 1	0.03	1.00	-0.38	0.33	0.01	0.29	-1.76	0.281	0.00	0.11	-0.09	0.25	0.02	0.61	-0.20	0.24
Age																
Step 2	0.07	2.86			0.16*	6.76			0.24**	11.03			0.128	5.09		
Age			-0.33	0.33			-0.120	0.217			-0.03	0.23			-0.16	0.23
Inhibitory Performance Score			-4.22	3.11			-6.13*	2.51			-6.48**	2.04			-4.28	2.34

\*  $P < 0.05$

\*\*  $P < 0.01$ .

Results are significant after FDR corrections.